

EE

LBL-36503  
UC-414



# Lawrence Berkeley Laboratory

UNIVERSITY OF CALIFORNIA

## Accelerator & Fusion Research Division

Presented at the 1995 Particle Accelerator Conference,  
Dallas, TX, May 1-5, 1995, and to be published in  
the Proceedings

### UV Laser Ionization and Electron Beam Diagnostics for Plasma Lenses

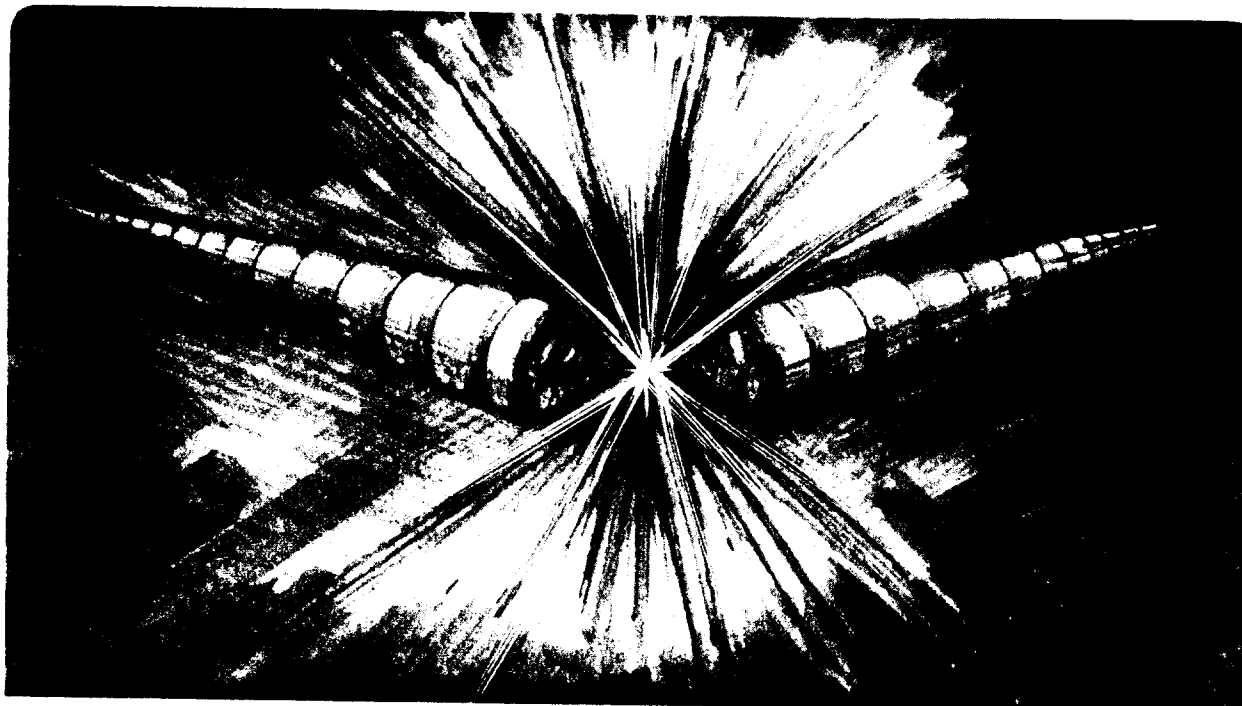
R. Govil, P. Volfbeyn, and W. Leemans

April 1995



SCAN-9509011

CERN LIBRARIES, GENEVA



W413

**UV LASER IONIZATION AND ELECTRON BEAM  
DIAGNOSTICS FOR PLASMA LENSES\***

R. Govil, P. Volfbeyn, and W. Leemans

Lawrence Berkeley Laboratory  
University of California  
Berkeley, California 94720

Submitted to the 1995 Particle Accelerator Conference and International Conference on  
High Energy Accelerators, Dallas, Texas,  
May 1 - 5, 1995

\* This work was supported by the Director, Office of Energy Research, Office of Basic Energy Sciences, Materials Sciences Division, of the U. S. Department of Energy, under Contract No. DE-AC03-76SF00098.

# UV LASER IONIZATION AND ELECTRON BEAM DIAGNOSTICS FOR PLASMA LENSES\*

R. Govil, P. Volfbeyn and W. Leemans, Lawrence Berkeley Laboratory, Berkeley CA 94720 USA

A comprehensive study of focusing of relativistic electron beams with overdense and underdense plasma lenses requires careful control of plasma density and scale lengths. Plasma lens experiments are planned at the Beam Test Facility of the LBL Center for Beam Physics, using the 50 MeV electron beam delivered by the linac injector from the Advanced Light Source. Here we present results from an interferometric study of plasmas produced in tri-propylamine vapor with a frequency quadrupled Nd:YAG laser at 266 nm. To study temporal dynamics of plasma lenses we have developed an electron beam diagnostic using optical transition radiation to time resolve beam size and divergence. Electron beam ionization of the plasma has also been investigated.

## I. INTRODUCTION

Plasma lenses [1] have been proposed for focusing relativistic electron beams to small spot sizes and for luminosity enhancement in future linear colliders. Plasma lenses can be overdense (plasma density,  $n_p$ , much greater than electron beam density,  $n_b$ ) or underdense ( $n_p < 2 n_b$ ). In overdense lenses the space-charge force of the electron beam is canceled by the plasma and the remaining magnetic force causes the electron beam to self-pinch. The focusing gradient is non-linear, resulting in spherical aberrations. In underdense lenses, the self-forces of the electron beam cancel, allowing the plasma ions to focus the beam. Such linear focusing (proportional to  $n_p$ ) leads to more desirable beam qualities. The performance of an underdense lens can be improved by tapering the plasma density in a such a way as to maximize the focusing strength at all times [2]. To avoid the Oide limit on spot sizes due to synchrotron radiation by the e-beam, adiabatic lenses have been proposed [3].

Overdense plasma lens focusing has been observed at the Argonne National Laboratory, at KEK and most recently at UCLA[4-6]. Only the UCLA experiment showed clear beam size reduction and the effect of temporal lens dynamics. To this date no experiments have been reported showing focusing of electron beams by plasma lenses operating in the underdense regime, nor has there been a systematic study of return currents, adiabatic lenses, etc.

## II. PLASMA LENS EXPERIMENT

The plasma lens experiment at the Beam Test Facility (BTF) is designed to study the properties of plasma lenses in both overdense and underdense regimes. In particular, we will

study important issues such as time response of the lens, lens aberrations and shot-to-shot reproducibility.

The Beam Test Facility provides a 50 MeV electron beam with a charge of 1-2 nC in 15 ps bunches at 1-10 Hz. The unnormalized emittance is 0.32 mm-mrad. The line is equipped with a wide range of diagnostics including integrating current transformers for charge measurement, high bandwidth BPMs, fluorescent screens, and optical transition radiation (OTR) diagnostics [7]. OTR is produced when electrons cross a boundary between materials of different dielectric constants. It can provide information about the electron beam energy (cone opening angle), bunch length, spot size and divergence (beam emittance).

### A. Plasma Lens Design

Using the nominal linac parameters, we have previously [8] determined the plasma requirements (density, location and length) and the e-beam requirements (size and charge) required for studying the different regimes. For a more realistic design, here we use experimentally measured electron beam properties. In addition, the following issues have been taken into consideration in designing the experiment.

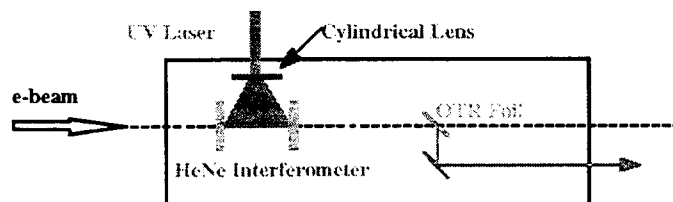


Figure 1. Experiment layout for adiabatic plasma lens. The laser is brought to a line focus at the position of the e-beam. Backward OTR is collected for electron beam diagnostics.

The plasma chamber is separated from the electron beam transport line by a  $3 \mu\text{m}$  beryllium window. For the overdense lens, the laser beam enters the vacuum chamber through an AR coated window and is made to propagate colinearly with the e-beam axis using an ultra-thin UV mirror ( $R=90\%$ ), made from  $5 \mu\text{m}$  nitrocellulose substrate. The substrate and Be-foil increase the e-beam emittance by 15-40%, in good agreement with calculations [9]. For the adiabatic lens (which requires better beam qualities), we avoid this emittance growth by bringing in the ionizing laser at right angles to the e-beam. The laser is brought to a line focus at the position of the electron beam. The plasma length will be adjusted by changing the laser focusing. The longitudinal profile of the plasma will be tapered using intensity or phase masks on the laser beam. Since the required change in density for planned adiabatic lenses is about an order of magnitude and the plasma

\* This work was supported by the Director, Office of Energy Research, Office of High Energy and Nuclear Physics, High Energy Physics Division, of the US Dept. Of Energy under Contract No. DE-AC03-76SF00098.

density varies as the square of intensity, the mask needs to provide a factor of 3 gradient in intensity.

Our calculations show that the contribution of beam induced ionization to the plasma density is negligible. Preliminary experimental observations made by propagating the electron beam through a 0.75 m long section filled to 2 Torr tri-propylamine (TPA) confirm this calculation.

Table 1. Typical overdense and underdense plasma lenses.

	Overdense	Adiabatic
<b>Electron Beam</b>		
Emittance [mm-mrad]	.32	.32
Charge [nC]	1.3	1.5
Initial density [ $10^{13} \text{ cm}^{-3}$ ]	.33	1.4
Initial size [microns]	139	113
<b>Plasma Parameters</b>		
Length [cm]	8.3	3.3
Density [ $10^{13} \text{ cm}^{-3}$ ]	1.0	0.2 - 3.2
<b>Electron Beam at Exit</b>		
Beam size [microns]	76	59
Overall size reduction factor	3.4	2.1

Overdense lenses require 5-15 cm long plasmas with densities ranging from  $8 \times 10^{12} - 2 \times 10^{13} \text{ cm}^{-3}$ . For example, a 5 cm long plasma placed 8 cm before vacuum focus of the e-beam, reduces the spot size from 187 microns to 63 microns. We find that for high plasma densities return currents play a significant role by canceling the effect of the lens. Sensitivity studies show that overdense lenses do not place very stringent requirements on the electron beam. A bunch charge of about 1.3 nC with emittance ranging from 0.3 to 0.5 mm-mrad is sufficient. Table 1 describes a typical overdense lens design.

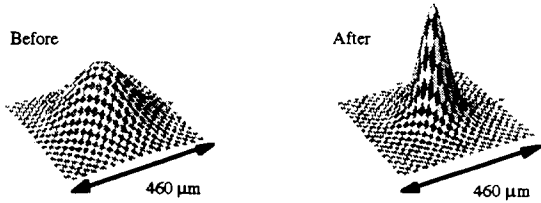


Figure 2a. Effect of plasma lens on transverse profile of electron beam. Here the z axis represents the charge density.

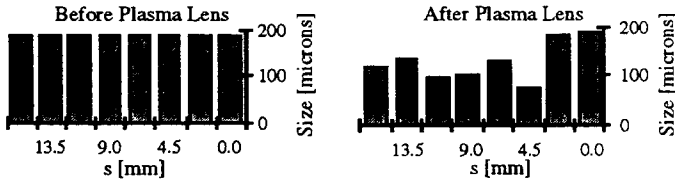


Figure 2b. Successive longitudinal slices of the e-beam experience different focusing strengths due to plasma response. Here s is the distance along the e-beam.

The focusing force in an underdense lens is proportional to the plasma density; since the plasma density has to be lower than the electron beam density, it is essential to achieve high e-beam density for high gradients and fast time response.

Description of a typical underdense adiabatic lens is given in Table 1. We find that (ignoring the temporal response of the plasma) a 15% drop in charge leads to a 5% drop in beam size reduction. A comparison between time-integrated and time-resolved effect of plasma lens focusing is shown in Fig. 2, clearly indicating the temporal modulation of the beam size.

### B. Plasma Production

Overdense and underdense plasmas are produced through resonant two-photon ionization of tri-propylamine (TPA) by a frequency quadrupled Nd:YAG laser at 266 nm. The plasmas produced through this method are field free and do not require magnetic confinement. TPA has a high vapor pressure (3.5 Torr) and a large ionization cross-section. Previously, we have measured the ionization cross-section of TPA at 248 nm using an Excimer KrF laser [8]. The plasma density as a function of neutral gas density  $N_o$  [ $\text{cm}^{-3}$ ] and laser intensity  $I$  [ $\text{W}/\text{cm}^2$ ] is given by [10]

$$n_p = \frac{N_o \alpha I^2 \Delta t}{h\nu} \quad (1)$$

Here  $\Delta t$  the FWHM of laser pulse [s],  $h\nu$  the photon energy [J] and  $\alpha$  the two-photon ionization coefficient [ $\text{cm}^4/\text{W}$ ]. The Nd:YAG provides 5 mm diameter pulses with about 100 mJ of energy at 266 nm in 7 - 9 ns (FWHM). Because the laser pulse length is short compared to the lifetime of the intermediate state, an alternate description of two-photon ionization may be more appropriate [10]:

$$n_p = \frac{N_o \sigma_1 \sigma_2 I^2 (\Delta t)^2}{2(h\nu)^2}, \quad (2)$$

where  $\sigma_1$  and  $\sigma_2$  are the cross-sections for photoexcitation of the intermediate level and for photoionization, respectively.

The plasma is diagnosed using 94.3 GHz microwave interferometry described previously [8]. The microwave signal is launched transversely to the plasma column. The line averaged plasma density (no attenuation or refraction included) is proportional to the microwave phase change:

$$\bar{n} = \frac{\int_0^L n(x) dx}{L} = \frac{2\epsilon_0 mc}{e^2} \omega \frac{\Delta\phi}{L}, \quad (3)$$

where  $\omega$  is the microwave frequency and  $\Delta\phi$  is the change in phase seen by the microwave signal.

Using the interferometer we have experimentally verified the pressure and intensity scaling laws as predicted by the two-photon ionization model (Fig. 3). Since the plasma sizes (3 - 5 mm diameter) are comparable to the microwave wavelength (3.2 mm), the plasma signal is modified by refraction. In addition, significant absorption of microwaves is observed at higher densities. The microwaves expand as they propagate through the plasma (which acts as a negative lens) and the receiving horn collects a smaller percentage of the transmitted waves, leading to a smaller relative signal. Thus the measured phase accumulation and, hence, the plasma density, is significantly smaller than its true value. Using plexiglass rods (which act as positive lenses and overfocus the

microwave beam) of varying diameters (4 - 6 mm), we have verified that refraction does lead to a significant modification to the collected signal. However, there is a way to bypass this problem. When the phase accumulation reaches  $90^\circ$ , the plasma signal turns around, retracing its steps past zero towards  $270^\circ$ . The signal at these "turning points" provides a measurement of phase, namely, at odd multiples of  $\pi/2$ , independent of the magnitude of the signal. An analysis of such points (Fig. 3b) reveals that the plasma density is in fact larger than it appears to be with refraction effects.

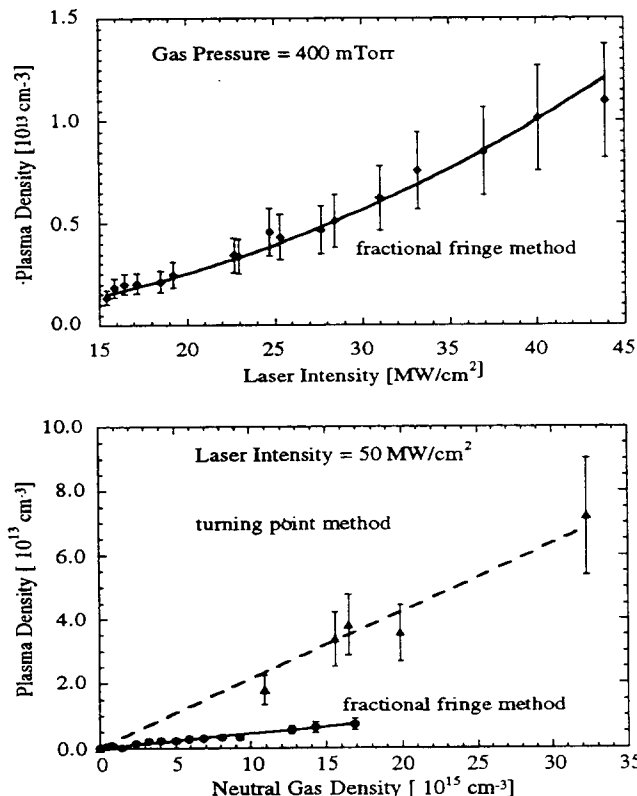


Figure 3. Plasma density scales (a) quadratically with intensity and (b) linearly with neutral gas density. The dashed curve is a measurement of density using the phase "turning point" method (at odd multiples of  $\pi/2$ ) described in Section IIB.

Laser intensity of 50 mJ in about 400 mTorr TPA produces  $3 \times 10^{13} \text{ cm}^{-3}$  plasma density, corresponding to 0.25% ionization efficiency. The ionization coefficient (Eq. 1) is found to be about  $8.24 \pm 2.4 \times 10^{-29} \text{ cm}^4/\text{W}$  compared to  $3 \times 10^{-26} \text{ cm}^4/\text{W}$  for 248 nm ionization reported earlier [8]. The corresponding value of  $\sqrt{\sigma_1 \sigma_2}$  (Eq. 2) is  $1.2 \pm 0.3 \times 10^{-19}$  compared to  $6 \times 10^{-19}$  reported by Woodworth et al. [10]. The actual plasma density may be higher because the turning point method may not fully account for plasma refraction and absorption. Slab plasmas will be produced through line focusing to resolve these issues. For diagnosing higher density plasmas required for adiabatic and tapered lenses and to achieve better spatial resolution, we are currently building a novel Fabry-Perot based optical interferometer at 633 nm, capable of measuring  $10^{14} - 10^{16} \text{ cm}^{-3}$  plasma densities with about  $50 \mu\text{m}$  spatial resolution.

### C. Electron Beam Diagnostics

To study the temporal dynamics of the plasma lens, it is necessary to time resolve the electron beam properties. Using a streak camera we have measured the electron beam spot size and divergence with 2 ps resolution at a location upstream of the plasma lens experiment. Fig. 4 shows a typical measurement of time-resolved beam divergence.

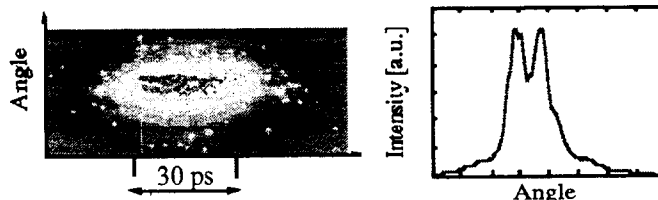


Figure 4. Beam divergence (proportional to ratio of "valley" to peak intensity) measured with 2 ps resolution.

At the plasma lens exit the electron beam properties will be measured using an OTR foil on a retractable arm moving along the direction of propagation of the e-beam (Fig. 1). This will allow us to image the electron beam at various location as it comes to a tight focus. Time resolved images of the electron beam will help determine the temporal response of the plasma.

## III. SUMMARY

A status report on the plasma lens experiment at BTF has been given, where a comprehensive study of over and underdense plasma lenses will take place. We have produced plasmas with densities varying from  $10^{12}$  to  $10^{14}$  through resonant two-photon ionization at 266 nm. Measured plasma densities agree with theoretical scaling laws with intensity and neutral gas pressure. Time-dependent e-beam emittance has been measured. Preliminary results show beam induced ionization of the gas fill to be insignificant. Design of intensity masks for producing tapered plasma profiles is in progress.

## IV. ACKNOWLEDGMENTS

The authors thank Glen Westenskow, Mike Perry and Bob Stever from LLNL for lending the Excimer and Nd:YAG laser systems and the microwave interferometer, respectively.

## V. REFERENCES

- [1] P. Chen, Part. Accel. **20**, 171 (1987).
- [2] T. Katsouleas et al., Proc. 1992 Adv. Accel. Workshop.
- [3] P. Chen et al., Phys. Rev. Lett. **64**, 1231 (1990).
- [4] J.B. Rosenzweig et al., Phys. Fluids **B2**, 1376 (1990).
- [5] H. Nakanishi et al., Phys. Rev. Lett. **66**, 1870 (1991).
- [6] G. Hairapetian et al., Phys. Rev. Lett. **72**, 2403 (1994).
- [7] M. de Loos et al., Proc. 1994 European Part. Accel. Conf.
- [8] W. Leemans et al., Proc. 1994 European Part. Accel. Conf.
- [9] M.B. Reid, J. Appl. Phys. **70**, 7185 (1991).
- [10] J. Woodworth et al., J. Appl. Phys. **57**, 1648 (1985).